Gadoxetate-enhanced Abbreviated MRI for Hepatocellular Carcinoma Surveillance: Preliminary Experience

Ryan L. Brunsing, MD, PhD • Dennis H. Chen, BSE • Alexandra Schlein, BS • Tanya Wolfson, MA •
Anthony Gamst, PhD • Adrija Mamidipalli, MBBS • Naik Vietti Violi, MD • Robert M. Marks, MD •
Bachir Taouli, MD • Rohit Loomba, MD, MHSc • Yuko Kono, MD, PhD • Claude B. Sirlin, MD

From the Liver Imaging Group, Department of Radiology, University of California San Diego, 200 W Arbor Dr, San Diego, CA 92103 (R.L.B., D.H.C., A.S., A.M., C.B.S.);
Computational and Applied Statistics Laboratory, San Diego Supercomputer Center, University of California San Diego, San Diego, Calif (T.W., A.G.); Department of
Radiology, Translational and Molecular Imaging Institute, Icahn School of Medicine at Mount Sinai, New York, NY (N.V.V., B.T.); Department of Radiology, Lausanne
University Hospital, Lausanne, Switzerland (N.V.V.); Department of Radiology, Naval Medical Center San Diego, Uniformed Services University of the Health Sciences,
Bethesda, Md (R.M.M.); Division of Epidemiology, Department of Family Medicine and Preventive Medicine, University of California San Diego, La Jolla, Calif (R.L.);
NAFLD Research Center, Department of Medicine, University of California San Diego, La Jolla, Calif (R.L.); and Department of Medicine and Radiology, University of
California San Diego, La Jolla, Calif (Y.K.). From the 2016 RSNA Annual Meeting. Received April 8, 2019; revision requested April 10; final revision received September 10;
accepted September 16. **Address correspondence to** C.B.S. (e-mail: *csirlin@ucsd.edu*).

Conflicts of interest are listed at the end of this article.

Purpose: To describe a single-center preliminary experience with gadoxetate disodium–enhanced abbreviated MRI for hepatocellular carcinoma (HCC) screening and surveillance in patients with cirrhosis or chronic hepatitis B virus (cHBV).

Materials and Methods: This was a retrospective study of consecutive patients aged 18 years and older with cirrhosis or cHBV who underwent at least one gadoxetate-enhanced abbreviated MRI examination for HCC surveillance from 2014 through 2016. Examinations were interpreted prospectively by one of six abdominal radiologists for clinical care. Clinical, imaging, and other data were extracted from electronic medical records. Diagnostic adequacy was assessed in all patients. Diagnostic accuracy was assessed in the subset of patients who could be classified as having HCC or not having HCC on the basis of a composite reference standard.

Results: In this study, 330 patients (93% with cirrhosis; 45% women; mean age, 59 years) underwent gadoxetate-enhanced abbreviated MRI. In the 330 patients, 311 (94.2%) baseline gadoxetate-enhanced abbreviated MRI examinations were diagnostically adequate. Of 141 (43%) of the 330 patients, 91.4% (129 of 141) could be classified as not having HCC and 8.6% (12 of 141) could be classified as having HCC. Baseline gadoxetate-enhanced abbreviated MRI had 0.92 sensitivity (95% confidence interval [CI]: 0.62, 1.00) and 0.91 specificity (95% CI: 0.84, 0.95) for detection of HCC. Of the 330 patients who underwent baseline gadoxetate-enhanced abbreviated MRI, 187 (57%) were lost to follow-up.

Conclusion: Gadoxetate-enhanced abbreviated MRI is feasible clinically, has a high diagnostic adequacy rate, and, on the basis of our preliminary experience, accurately depicts HCC in high-risk patients. Strategies to enhance follow-up compliance are needed.

Supplemental material is available for this article.

© RSNA, 2019++_++_

Hepatocellular carcinoma (HCC) is the most common primary liver malignancy, a leading cause of cancer death worldwide, and the most rapidly rising cause of cancer-related mortality in the United States (1). Cirrhosis and chronic hepatitis B virus (cHBV) infection without cirrhosis are major risk factors for HCC (2,3). Patients with symptoms at presentation usually have advanced disease and a dismal prognosis (4). By comparison, patients with early disease can be treated with curative intent (5). This finding has prompted the development of surveillance programs aimed at early detection of HCC in at-risk populations.

The only prospective randomized controlled trial assessing imaging-based HCC surveillance demonstrated that semiannual liver US combined with serum α-fetoprotein reduced HCC-related mortality by 37% (6). Because US has limited sensitivity for detecting early-stage HCC (7), alternative surveillance methods have been sought. Although MRI is more accurate in detecting HCC (8), MRI is suboptimal for HCC surveillance because of cost, long examination time, and complexity. To address this limitation, abbreviated MRI protocols using a reduced number of sequences are being developed (9–12) with the goal of driving down acquisition time while leveraging the detection accuracy of MRI. This general strategy has previously shown utility in MRI-based breast cancer screening (13).

One approach for detection of HCC is gadoxetate disodium–enhanced abbreviated MRI, which uses three complementary sequences: a hepatobiliary phase (HBP) T1-weighted sequence to depict HCC nodules based on altered expression of the OATP1B3 transporter responsible for uptake of gadoxetate into hepatocytes (14,15), a diffusion-weighted imaging (DWI) sequence to improve sensitivity by depicting HCC nodules based on high cellularity (16,17) independent of OATP1B3 expression, and a T2-weighted single-shot fast spin-echo sequence to improve specificity by excluding benign cysts and hemangiomas (18), which may resemble

Abbreviations

cHBV = chronic hepatitis B virus, CI = confidence interval, DWI = diffusion-weighted imaging, HBP = hepatobiliary phase, HBV = hepatitis B virus, HCC = hepatocellular carcinoma, HCV = hepatitis C virus, iMELD = integrated Model for End-stage Liver Disease, LI-RADS = Liver Imaging Reporting and Data System, NAFLD = nonalcoholic fatty liver disease, NPV = negative predictive value, PPV = positive predictive value

Summary

Gadoxetate-enhanced abbreviated MRI can be implemented clinically with high diagnostic adequacy in the setting of compromised US surveillance; preliminary analysis of a subcohort of 141 patients demonstrated high sensitivity and negative predictive value in detecting hepatocellular carcinoma (HCC) in high-risk patients when interpreted prospectively in a subspecialty clinical service, but, as with other HCC surveillance programs, the loss-to-follow-up rate was high.

Key Points

- Gadoxetate-enhanced abbreviated MRI can be implemented clinically with a high diagnostic adequacy rate.
- Preliminary analysis suggests that gadoxetate-enhanced abbreviated MRI accurately depicts hepatocellular carcinoma (HCC) in high-risk patients with 0.92 sensitivity, 0.91 specificity, and overall accuracy of 0.91, but, as with other HCC surveillance programs, the loss-to-follow-up rate is high.
- Abbreviated MRI may provide a viable method for HCC surveillance in high-risk patients, especially if strategies to enhance follow-up compliance are developed.

HCC in the other sequences. Gadoxetate-enhanced abbreviated MRI has several time-saving advantages: It streamlines workflow by allowing injection of contrast material while the patient is in the waiting area, requires little imaging system time, and uses few sequences with structured reporting to simplify interpretation. One analysis suggested gadoxetate-enhanced abbreviated MRI could offer substantial cost savings over conventional MRI (10), and another analysis suggested that in real-world circumstances it may be the most cost-effective approach (19).

Previous work has demonstrated gadoxetate-enhanced abbreviated MRI can accurately depict HCC when retrospectively simulated (10,12), but those studies were interpreted in a research setting, included patients with known or suspected HCC, did not reflect a true surveillance population, and tended to have patients with more advanced cancer, and so may have inflated the observed performance. No study has evaluated the accuracy of gadoxetate-enhanced abbreviated MRI when performed and reported prospectively in a surveillance population or in the clinical setting. In 2014, our institution began offering gadoxetate-enhanced abbreviated MRI-based surveillance for HCC in high-risk patients in whom US screening was compromised by obesity, hepatic steatosis, or severe parenchymal heterogeneity, as determined by the ordering hepatologist. Here we describe our preliminary experience with this protocol, including a retrospective assessment of the feasibility, diagnostic adequacy, and diagnostic accuracy of clinically implemented gadoxetate-enhanced abbreviated MRI for the detection of HCC in a high-risk population.

Materials and Methods

Patient Identification: Total Cohort

In 2014, our institution began offering gadoxetate-enhanced abbreviated MRI-based surveillance for HCC in high-risk patients in whom US screening was compromised by obesity, hepatic steatosis, or severe parenchymal heterogeneity. Examinations required a 10–15-minute imaging time and were performed with a 50% charge reduction by using a limited examination code modifier. This single-center retrospective study with cross-sectional and longitudinal components was compliant with the Health Insurance Portability and Accountability Act and approved by the institutional review board with an informed consent waiver. Using a cloud-based engine (M*Modal Catalyst; Franklin, Tenn), our institutional radiology information system was searched by one author (a senior radiology resident; R.L.B.) to identify all patients who underwent at least one gadoxetate-enhanced abbreviated MRI examination between May 1, 2014, and December 31, 2016.

Consecutive patients meeting the following eligibility criteria were enrolled in the study and included in the analysis of diagnostic adequacy of gadoxetate-enhanced abbreviated MRI (Fig 1). Inclusion variables included the following: (a) age 18 years old and older, (b) gadoxetate-enhanced abbreviated MRI radiology report completed, and (c) cirrhosis of any etiology and noncirrhotic cHBV. Exclusion variables were as follows: (a) diagnosis of cirrhosis or noncirrhotic hepatitis B virus (HBV) could not be verified, retrospectively; (b) gadoxetate-enhanced abbreviated was MRI performed for a reason other than HCC surveillance; (c) known primary or secondary liver cancer; and (d) vascular cause of liver disease (Budd-Chiari syndrome) for which the Liver Imaging Reporting and Data System (LI-RADS) does not apply (20).

Patient Identification: Subcohort for Diagnostic Performance

Enrolled patients were included in the analysis of diagnostic performance if they could be classified as "positive for HCC" or "negative for HCC" by using the composite reference standard described below. Patients who were considered "indeterminate for HCC" or "positive for other malignancy" were excluded from this analysis. The latter were excluded because according to clinical practice guidelines (21–23), surveillance programs were intended to detect HCC, not other malignancies.

Reference Standard for Assessing Diagnostic Performance

A composite reference standard was applied at the per-patient level. Blinded to the gadoxetate-enhanced abbreviated MRI results, the senior resident reviewed each patient's results of the following tests through September 31, 2017: follow-up surveillance US examinations; multiphase CT or MRI examinations reported by using LI-RADS, version 2014 (24) or version 2017 (25); and histopathologic reports. The resident also

recorded the dates and types of any subsequent treatments for presumptive HCC by consensus decision of the multidisciplinary tumor board.

Prior to data analysis, the reference standard was classified as follows:

1. Positive for other malignancy if a non-HCC malignancy was confirmed histologically within 365 days after gadoxetate-enhanced abbreviated MRI;

2. Positive for HCC if not positive for other malignancy AND if *(a)* follow-up multiphase CT or MRI was performed fewer than 365 days after abbreviated MRI showed at least one LI-RADS 5 observation OR *(b)* follow-up multiphase CT or MRI examination performed fewer than 365 days after gadoxetate-enhanced abbreviated MRI showed at least one LI-RADS 4 observation subsequently treated as presumptive HCC by consensus decision of the multidisciplinary tumor board, OR *(c)* HCC was confirmed histologically within 365 days after gadoxetate-enhanced abbreviated MRI. The location of the HCC in positive cases was retrospectively reviewed by two reviewers (R.L.B. and C.B.S.) in consensus and was confirmed to match the abbreviated MRI lesion.

3. Confirmed as negative for malignancy if it was not positive for other malignancy or HCC AND *(a)* if multiphase CT or MRI performed after gadoxetate-enhanced abbreviated MRI showed no reportable observation or only LI-RADS 1 and/or LI-RADS 2 observations OR *(b)* the highest categorized observation on any multiphase CT or MRI examination performed after baseline gadoxetate-enhanced abbreviated MRI was LI-RADS 3 or LI-RADS 4 without subsequent treatment OR *(c)* if explant histologic findings at any time after gadoxetate-enhanced abbreviated MRI were negative for malignancy OR *(d)* if surveillance US performed 365 days or more after baseline gadoxetate-enhanced abbreviated MRI was reported as negative.

4. Lesions were considered indeterminate for HCC if they were not classified in one of the previous three categories. This included patients without follow-up multiphase CT or MRI examinations, patients with multiphase CT or MRI with a LI-RADS M observation with inconclusive work-up, patients whose only follow-up was negative or subthreshold gadoxetate-enhanced abbreviated MRI, and patients whose only follow-up was positive gadoxetate-enhanced abbreviated MRI that could not be classified in one of the previous three categories.

After the reference standard classification was locked, one author (R.L.B.) retrospectively reviewed follow-up multiphase CT or MRI examinations in conjunction with the baseline gadoxetate-enhanced abbreviated MRI examinations in
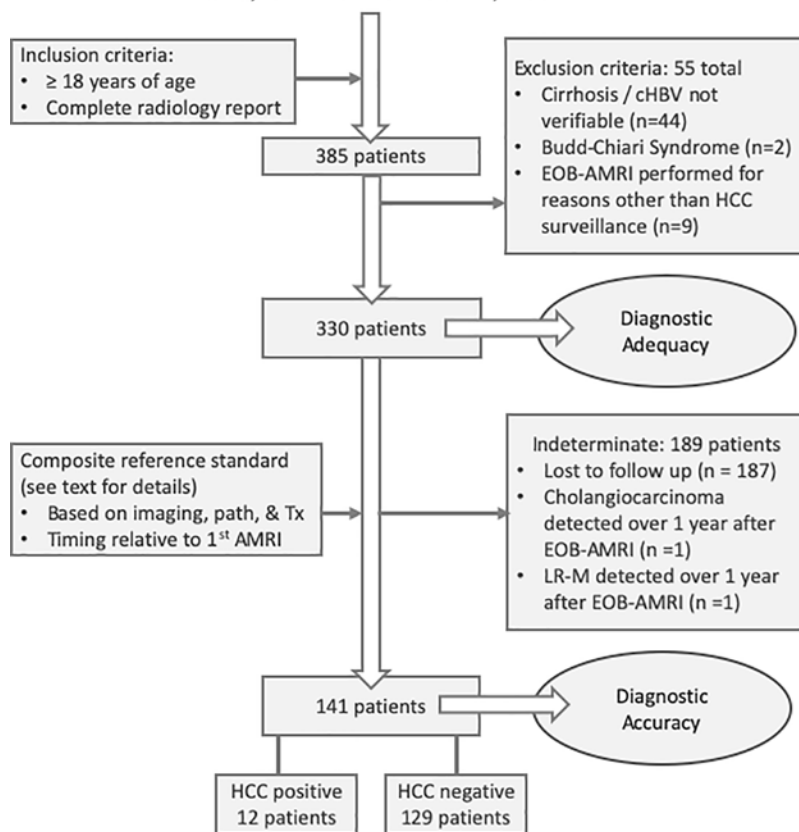

Figure 1: Schematic diagram of patient selection process. A search of our institutional database revealed 385 patients 18 years or older who had undergone at least one gadoxetate-enhanced (EOB) abbreviated MRI (AMRI) examination from 2014 to 2016, including a completed radiology report. Of these 385 patients, 55 were excluded. In total, 330 patients with cirrhosis or chronic hepatitis B virus (cHBV) without cirrhosis were included in our cross-sectional and longitudinal assessment of the technical performance of gadoxetate-enhanced abbreviated MRI, including the rates of inadequate and positive studies. We then applied a composite reference standard and identified a subset of patients who could be classified as either hepatocellular carcinoma (HCC) positive (12 patients) or HCC negative (129 patients). Details of the composite reference standard are included in the Materials and Methods section. LR-M = probably or definitely malignant, not specific for HCC; Tx = treatment.

HCC-positive patients to assess lesion-level correspondence of abbreviated MRI–detected observations and HCC nodules. All CT and MRI examinations performed in follow-up of gadoxetate-enhanced abbreviated MRI findings adhered to the most recent LI-RADS technical requirements available at the time of the examination, either LI-RADS, version 2014 or CT/MRI LI-RADS, version 2017.

Abbreviated MRI Examination Technique

Gadoxetate-enhanced abbreviated MRI examinations were performed on 1.5 T (Signa HDx, GE Healthcare, Waukesha, Wis) or 3.0 T (Signa HDxt and 750w, GE Healthcare, Waukesha, Wis) systems for clinical care by using a protocol as described in a prior simulation study (10). In brief, it included axial DWI with apparent diffusion coefficient maps, axial T2-weighted single-shot fast spin-echo imaging, and axial T1-weighted three-dimensional gradient-echo fat-suppressed HBP imaging following administration of 0.025 mg/
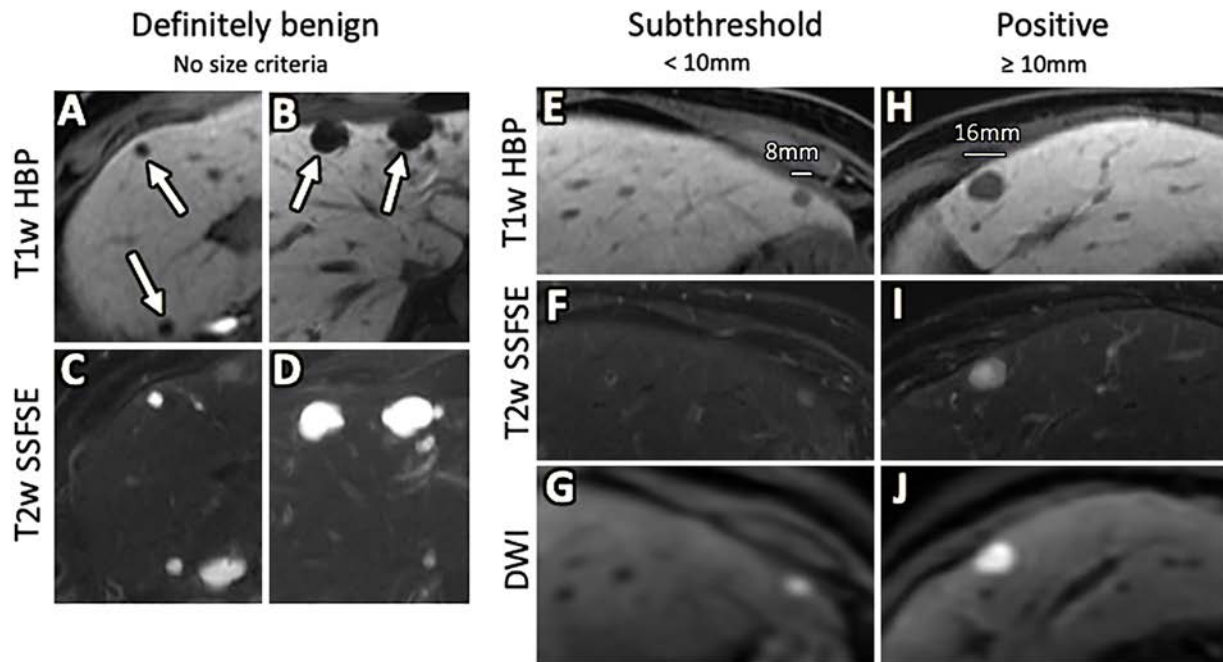
Figure 2: Gadoxetate-enhanced abbreviated MRI interpretation. *A–D,* Examples of definitely benign observations, as called by the interpreting radiologist; arrows = well-circumscribed markedly hypointense observations on, *A, B,* T1-weighted hepatobiliary phase (T1w HBP) images which correspond to markedly T2 hyperintense observations on, *C, D,* T2-weighted single-shot fast spin-echo (T2w SSFSE) images, compatible with benign cysts. *E–G,* Example of subthreshold observation; an 8-mm observation in the lateral section is moderately hypointense, *E,* on the T1-weighted HBP image, mild to moderately hyperintense, *F,* on the T2-weighted SSFSE and demonstrates high signal, *G,* on diffusion-weighted imaging (DWI), suggesting restricted diffusion. Because the observation is smaller than 10 mm, it qualifies the study as subthreshold. *H–J,* Example of positive observation; a 16-mm observation in the lateral section is moderately hypointense, *H,* on the T1-weighted HBP image, mildly to moderately hyperintense, *I,* on the T2-weighted SSFSE image and demonstrates high signal at DWI, suggesting restricted diffusion, *I.* Because the observation is greater than or equal to 10 mm in size, it qualifies the study as positive. Note that our current clinical practice is to consider only HBP T1-weighted hypointense observations and/or DWI-hyperintense observations as grounds for a subthreshold or positive scoring after exclusion of benign entities. T1-weighted HBP = T1-weighted three-dimensional gradient-echo fat-suppressed imaging acquired 20 minutes following administration of 0.025 mmol/kg gadoxetic disodium, T2-weighted SSFSE = T2-weighted single-shot fast spin-echo imaging.

kg gadoxetate disodium (Bayer; Whippany, NJ). Sequences and parameters are listed in Appendix E1 (supplement).

Abbreviated MRI Reporting

Gadoxetate-enhanced abbreviated MRI examinations were read for clinical care by using a standardized report template (completed by one of six abdominal imaging faculty members, each with postfellowship experience ranging from < 1 year to > 30 years). Guidelines on interpreting gadoxetate-enhanced abbreviated MRI have been previously reported (10). Each examination was scored on a four-point scale (Fig 2).

A negative result indicated no focal observations or only definitely benign observations. The determination of "definitely benign" was a judgment call made by the interpreting radiologist and included sharply demarcated lesions with marked T2 hyperintensity interpreted as cysts or hemangiomas. Nodules with HBP hyperintensity were also considered negative unless they showed restricted diffusion or other suspicious features such as a nodule-in-nodule appearance.

A subthreshold result indicated one or more observations not definitely benign and demonstrating HBP hypointensity, restricted diffusion, and/or other suspicious features such as nodule-in-nodule appearance, all measuring less than 10 mm.

A positive result indicated one or more observations not definitely benign and demonstrating HBP hypointensity, restricted diffusion, and/or other suspicious features such as nodule-in-nodule appearance, with at least one measuring 10 mm or greater.

An inadequate result indicated not positive and HBP images severely limited by impaired liver enhancement, motion artifact, dielectric artifact from ascites, or other factor.

Retrospective Abbreviated MRI Rescoring

Prior to March 1, 2015, we used a three-point system that did not include the subthreshold score. As experience accrued, we learned that gadoxetate-enhanced abbreviated MRI–detected suspicious observations of less than 10 mm were rarely malignant; thus, a subthreshold category was added. For this research study, gadoxetate-enhanced abbreviated MRI examinations reported clinically as positive were retrospectively rescored as subthreshold if the largest reported observation was less than 10 mm. This assessment was based on lesion sizes reported by the interpreting radiologist. Images were not reinterpreted. In total, six cases were rescored.

Data Collection

See Appendix E1 (supplement).

Statistical Analysis

Statistical analyses were performed by using R, version 3.3.1 (the R Foundation for Statistical Computing, Vienna, Austria, 2016).

Study flow, screening rates, interval between successive follow-up examinations, and proportion of positive and (positive and subthreshold) examinations were graphically summarized. Cohort characteristics and baseline gadoxetate-enhanced abbreviated MRI categories (including inadequate examinations) were summarized. To assess whether liver function affected image interpretation, integrated Model for End-stage Liver Disease (iMELD) (26) and Child-Pugh scores were compared between patients grouped by the result of their baseline gadoxetate-enhanced abbreviated MRI examination. Bonferroni correction for multiple comparisons was applied to each score. Only iMELD and Child-Pugh scores acquired within 6 months of the baseline gadoxetate-enhanced abbreviated MRI examination were included in this analysis.

To evaluate performance of gadoxetate-enhanced abbreviated MRI for detecting HCC, baseline gadoxetate-enhanced abbreviated MRI scores were tabulated against reference standard classifications. Gadoxetate-enhanced abbreviated MRI scores were dichotomized in three ways: (a) positive versus subthreshold, negative, or inadequate; (b) positive or subthreshold versus negative or inadequate; and (c) positive versus subthreshold or negative, excluding inadequate.

Reference standard classifications were dichotomized as HCC versus negative; other malignancies were excluded from the analysis, as explained previously. Sensitivity, specificity, positive predictive value (PPV), negative predictive value (NPV), and total accuracy were estimated. Exact binomial confidence intervals were computed for each parameter. Accuracy of follow-up surveillance gadoxetate-enhanced abbreviated MRI examinations was not assessed. Cancer detection rate was estimated from the number of HCC-positive patients revealed at baseline gadoxetate-enhanced abbreviated MRI screening (n = 11) and the number of baseline examinations required for the detection (n = 330). It was reported in terms of HCC detected per 1000 examinations.

Results

Diagnostic Adequacy Cohort

Of 385 patients meeting the inclusion criteria, 45 were excluded. Of the remaining 330 patients, 149 (45%) were women with cirrhosis or cHBV infection in our cohort (Fig 1) for assessing the diagnostic adequacy of gadoxetate-enhanced abbreviated MRI. Diagnostic adequacy cohort characteristics are summarized in Table 1. Whites (51.2%), Hispanics or Latinos (23.0%), Asians (12.7%), and blacks (3.9%) comprised the largest racial groups.

Of 330 patients, 308 (93.3%) had cirrhosis (see Appendix E1 [supplement]), whereas 22 (6.7%) had cHBV without cirrhosis (Table 1). The most common etiologies of cirrhosis were hepatitis C virus (HCV) (41.2%), alcohol (19.5%), nonalcoholic fatty liver disease (NAFLD) (12.3%), and HBV (6.8%).

Sixteen patients (nine men, seven women) had missing data required for calculation of iMELD and Child-Pugh scores.

Diagnostic Accuracy Subcohort

Of the 330 patients in the overall cohort used for assessing diagnostic adequacy, the reference standard was deemed "indeterminate for HCC" in 189 of 330 patients: 187 patients were lost to follow-up and two patients had tumors detected more than 365 days after gadoxetate-enhanced abbreviated MRI (one patient with a LI-RADS M observation at follow-up MRI without further evaluation; one patient with a biopsy-proven cholangiocarcinoma). No patient was excluded for having positive findings for other malignancy within 365 days. The remaining 141 patients were included in the accuracy analysis; 91.4% (129 of 141) were HCC negative and 8.6% (12 of 141) were HCC positive (Fig 1). Diagnostic accuracy cohort characteristics are summarized in Table 1. The HCC-positive group included nine patients with LI-RADS 5 lesions and three patients with LI-RADS 4 lesions treated as presumptive HCC by consensus decision of the multidisciplinary tumor board. The average time from gadoxetate-enhanced abbreviated MRI to diagnosis was 80 days (range, 4–248 days; Table E1 [supplement]). All 12 patients had cirrhosis. The HCC-negative group included three patients with LI-RADS 4 observations (Table 2), all of which were detected more than 365 days following gadoxetate-enhanced abbreviated MRI (mean, 625 days; range, 581–700 days) and 11 patients whose highest category observation was LI-RADS 3.

Baseline Gadoxetate-enhanced Abbreviated MRI Diagnostic Adequacy

Of 330 baseline gadoxetate-enhanced abbreviated MRI examinations, 7.3% (24 of 330) were positive, 3.3% (11 of 330) were subthreshold, 83.6% (276 of 330) were negative, and 5.8% (19 of 33) were inadequate (Table 3). Thus, 311 (94.2%) of the 330 examinations were adequate. All 19 patients with inadequate abbreviated MRI had cirrhosis, and 15 of the 19 patients had impaired HBP uptake (Table 4). The mean body mass index was trendwise (P = .18) lower for inadequate (average, 27.7 kg/m²; range, 18.8–40.2 kg/m²) than for adequate (average, 29.2 kg/m²; range, 14.6–49.5 kg/m²) examinations.

Compared with those patients with a negative gadoxetate-enhanced abbreviated MRI examination, patients with an inadequate gadoxetate-enhanced abbreviated MRI examination had significantly higher iMELD scores (12.6 vs 9.2; P = .0007, Fig 3a) and Child-Pugh scores (7.4 vs 5.6; P = .0006, Fig 3b). Similar trends were noted between the inadequate group and both the positive and subthreshold groups, but these were not significant, possibly the result of small group sizes. These scores did not differ in pairwise comparisons of patients with a positive, subthreshold, or negative gadoxetate-enhanced abbreviated MRI examination (P > .05 for all) (Fig 3).

Compared with those patients with positive, subthreshold, or negative examinations, patients with an inadequate gadoxetate-enhanced abbreviated MRI examination nominally were more likely to have ascites (17% vs 44%), impaired HBP enhancement (9% vs 89%), or liver parenchymal heterogeneity (62% vs 83%) (Table 3), but formal statistical analyses were not performed.

Baseline Gadoxetate-enhanced Abbreviated MRI Diagnostic Accuracy

Of the 12 patients with HCC, 11 had a positive and one had a negative baseline gadoxetate-enhanced abbreviated MRI exam-

Table 1: Patient Demographics

Characteristic	Diagnostic Adequacy Cohort	Diagnostic Accuracy Cohort
Demographic data		
No. of patients (% cohort)	330 (100)	141 (100)
Mean age (y) ± standard deviation	59.4 ± 10.9	59.1 ± 11.5
Mean BMI (kg/m²) ± standard deviation	29.1 ± 5.9	29.3 ± 5.8
No. of women	149 (45.1)	64 (45.4)
Ethnicity		
Non-Hispanic	224 (67.9)	94 (66.7)
Hispanic	98 (29.7)	46 (32.6)
Not known	8 (2.4)	1 (0.7)
Race		
American Indian/Alaskan Native	3 (0.9)	2 (1.4)
Asian	42 (12.7)	15 (10.6)
Black or African American	13 (3.9)	8 (5.7)
Hispanic or Latino	76 (23.0)	31 (22.0)
Native Hawaiian/Pacific Islander	1 (0.3)	1 (0.7)
White	169 (51.2)	71 (50.4)
Other	19 (5.8)	12 (8.5)
Unknown	7 (2.1)	1 (0.7)
Liver disease		
Chronic hepatitis B without cirrhosis	22 (6.7)	10 (7.1)
Cirrhosis	308 (93.3)	131 (92.9)
Hepatitis C virus	127 (38.5)	60 (42.6)
Alcohol	60 (18.2)	25 (17.7)
Nonalcoholic fatty liver disease	38 (11.5)	13 (9.2)
Hepatitis B virus	21 (6.4)	8 (5.7)
Cryptogenic	17 (5.2)	7 (5.0)
Autoimmune hepatitis	15 (4.5)	6 (4.3)
Primary biliary cirrhosis	4 (1.2)	0 (0)
Primary sclerosing cholangitis	2 (0.6)	2 (1.4)
Alpha-1 antitrypsin deficiency	1 (0.3)	0 (0)
Wilson disease	1 (0.3)	1 (0.7)
Hemochromatosis	0 (0)	0 (0%)
More than one etiology	22 (6.7)	9 (6.4)
Severity of liver disease*		
Child-Pugh A	258 (82.2)	110 (78.0)
Child-Pugh B	47 (15.0)	21 (14.9)
Child-Pugh C	9 (2.9)	7 (5.0)
Mean Child-Pugh score ± standard deviation	5.8 ± 1.3	5.8 ± 1.5
Mean iMELD score ± standard deviation	9.5 ± 3.1	9.6 ± 3.5
Other laboratory data†‡		
Mean AST (U/L) ± standard deviation	45.8 ± 37.3	47.9 ± 36.2
Mean ALT (U/L) ± standard deviation	36.3 ± 32.8	36.5 ± 28.8
Mean albumin (g/dL) ± standard deviation	3.9 ± 0.6	3.9 ± 0.6
Mean total bilirubin (mg/dL) ± standard deviation	1.1 ± 1.3	1.3 ± 1.8
Mean serum sodium (mEq/L) ± standard deviation	139.2 ± 3.3	139.2 ± 3.2
Mean INR ± standard deviation	1.2 ± 0.2	1.2 ± 0.2
Mean creatinine (mg/dL) ± standard deviation	0.9 ± 0.3	0.9 ± 0.3
Mean platelets (K/µL) ± standard deviation	130.2 ± 64.4	127.0 ± 64.1

Note.—Unless otherwise indicated, data are numbers of patients, with percentages in parentheses. ALT = alanine aminotransferase, AST = aspartate aminotransferase, BMI = body mass index, iMELD = integrated Model for End-stage Liver Disease, INR = international normalized ratio.
* 15 patients were missing INR ± additional laboratory data, no iMELD/Child-Pugh score.
† Three patients were missing AST/ALT levels.
‡ 15 patients were missing platelets.

Table 2: Reference Standard Classification for Each Baseline Gadoxetate-enhanced Abbreviated MRI Score

Parameter	No. of Patients	Percentage of All Patients	Reference Standard Classification
Positive baseline abbreviated MRI	24	7.3	
F/U US/CT/MR negative	8	2.4	Negative for HCC
F/U CT/MR–LI-RADS 3	4	1.2	Negative for HCC
F/U CT/MR–LI-RADS 4, not treated or biopsied within 365 days	0	0	Negative for HCC
F/U CT/MR–LI-RADS 4, treated as presumptive HCC within 365 days	4	1.2	Positive for HCC
F/U CT/MR–LI-RADS 5	7	2.1	Positive for HCC
F/U CT/MR–LI-RADS M, not treated or biopsied within 365 days	0	0	Indeterminate for HCC
Biopsy-proven non-HCC malignancy	0	0	Positive for OM–excluded
Insufficient data or lost to follow-up	1	0.3	Indeterminate for HCC
Subthreshold baseline abbreviated MRI	11	3.3	
F/U US/CT/MR negative	7	2.1	Negative for HCC
F/U CT/MR–LI-RADS 3	1	0.3	Negative for HCC
F/U CT/MR–LI-RADS 4, not treated or biopsied within 365 days	0	0	Negative for HCC
F/U CT/MR–LI-RADS 4, treated as presumptive HCC within 365 days	0	0	Positive for HCC
F/U CT/MR–LI-RADS 5	0	0	Positive for HCC
F/U CT/MR–LI-RADS M, not treated or biopsied within 365 days	0	0	Indeterminate for HCC
Biopsy-proven non-HCC malignancy	0	0	Positive for OM–excluded
Insufficient data or lost to follow-up	3	0.9	Indeterminate for HCC
Negative baseline abbreviated MRI	276	83.6	
F/U US/CT/MR negative	85	25.8	Negative for HCC
F/U CT/MR–LI-RADS 3	6	1.8	Negative for HCC
F/U CT/MR–LI-RADS 4, not treated or biopsied within 365 days	3	0.9	Negative for HCC
F/U CT/MR–LI-RADS 4, treated as presumptive HCC within 365 days	0	0	Positive for HCC
F/U CT/MR–LI-RADS 5	1	0.3	Positive for HCC
F/U CT/MR–LI-RADS M, not treated or biopsied within 365 days	1	0.3	Indeterminate for HCC
Biopsy-proven non-HCC malignancy	1	0.3	Positive for OM–excluded
Insufficient data or lost to follow-up	179	54.2	Indeterminate for HCC
Inadequate baseline abbreviated MRI	19	5.8	
F/U US/CT/MR negative	15	4.5	Negative for HCC
F/U CT/MR–LI-RADS 3	0	0	Negative for HCC
F/U CT/MR–LI-RADS 4, not treated or biopsied within 365 days	0	0	Negative for HCC
F/U CT/MR–LI-RADS 4, treated as presumptive HCC within 365 days	0	0	Positive for HCC
F/U CT/MR–LI-RADS 5	0	0	Positive for HCC
F/U CT/MR–LI-RADS M, not treated or biopsied within 365 days	0	0	Indeterminate for HCC
Biopsy-proven non-HCC malignancy	0	0	Positive for OM–excluded
Insufficient data or lost to follow-up	4	1.2	Indeterminate for HCC

Note.—F/U = follow-up, HCC = hepatocellular carcinoma, LI-RADS = Liver Imaging Reporting and Data System, OM = malignancy other than HCC.

ination; none had a subthreshold gadoxetate-enhanced abbreviated MRI examination. In each of the 11 patients with HCC and a positive baseline examination, the observation detected by gadoxetate-enhanced abbreviated MRI corresponded with an HCC nodule as defined previously. This correlated to a cancer detection rate of 37 HCCs per 1000 gadoxetate-enhanced abbreviated MRI examinations. See Tables 3 and 4. Of the 11 patients with HCC depicted by gadoxetate-enhanced abbreviated MRI, one patient (patient 6) had two LI-RADS 5 lesions measuring 45 and 27 mm. Another patient (patient 222) had a 10-mm HBP hypointense nodule representing potentially curable disease on baseline gadoxetate-enhanced abbreviated MRI. In retrospect, the lesion had subtle arterial phase hy-perenhancement and washout appearance (ie, LI-RADS 5 by LI-RADS, version 2018) at call-back multiphase MRI 34 days later, but the lesion was missed due in part to arterial phase mistiming; this patient was subsequently lost to follow-up for 1.5 years when repeat MRI showed interval growth of the lesion into a 87-mm mass with tumor in vein. The remaining nine patients either had LI-RADS 5 lesions meeting the Milan criteria (27) or some combination of LI-RADS 3/LI-RADS 4 lesions. Thus, all nine of these patients were potentially curable. Details about lesion size and follow-up in the HCC-positive population can be found in Table E1 (supplement). Figure 4 is an example of a 15-mm lesion detected with gadoxetate-enhanced abbreviated MRI, subsequently shown to

Table 3: Baseline Abbreviated MRI Results

Baseline Abbreviated MRI Result	Total	Nodularity*	Ascites†	Impaired HBP‡	Parenchymal Heterogeneity§
Positive	24/330 (7.3)	24/24 (100)	5/24 (20.8)	2/22 (9.1)	17/22 (77.2)
Subthreshold	11/330 (3.3)	10/11 (90.9)	2/11 (18.2)	2/10 (20.0)	7/10 (70)
Negative	276/330 (83.6)	254/271 (93.7)	44/270 (16.3)	23/257 (8.0)	155/256 (60.5)
Inadequate	19/330 (5.8)	18/18 (100)	8/18 (44.4)	16/18 (88.9)	15/18 (83.3)
Total	330/330 (100)	306/324 (94.4)	59/323 (17.9)	43/307 (13.0)	194/306 (58.8)

Note.—Unless otherwise specified, data are numbers of patients, with percentages in parentheses. HBP = hepatobiliary phase.
* Presence or absence of surface nodularity was reported for 324 of 330 patients.
† Presence or absence of ascites was reported for 323 of 330 patients.
‡ Presence or absence of impaired HBP enhancement was reported for 307 of 330 patients.
§ Presence of absence of liver parenchymal heterogeneity was reported for 306 of 330 patients.

be LI-RADS 5 at diagnostic MRI. The lone patient with HCC and a negative baseline examination was a 55-year-old man with HCV cirrhosis who underwent a multiphase MRI examination 187 days after his gadoxetate-enhanced abbreviated MRI examination and was found to have HCC by imaging criteria with tumor in vein (LI-RADS-TIV). He was subsequently treated with radioembolization. Of the 129 patients without HCC, eight had positive, 99 had negative, seven had subthreshold, and 15 had an inadequate gadoxetate-enhanced abbreviated MRI examination.

Positive gadoxetate-enhanced abbreviated MRI provided a sensitivity of 0.92 (95% confidence interval [CI]: 0.62, 1.00), a specificity of 0.91 (95% CI: 0.84, 0.95), an NPV of 0.99 (95% CI: 0.94, 1.00), a PPV of 0.48 (95% CI: 0.27, 0.69), and an accuracy of 0.91 (95% CI: 0.85, 0.95). See Table 5.

Positive or subthreshold gadoxetate-enhanced abbreviated MRI provided a sensitivity of 0.92 (95% CI: 0.62, 1.00), a specificity of 0.85 (95% CI: 0.77, 0.90), an NPV of 0.99 (95% CI: 0.95, 1.00), a PPV of 0.36 (95% CI: 0.19, 0.55), and an accuracy of 0.85 (95% CI: 0.78, 0.91).

After exclusion of the inadequate studies, positive gadoxetate-enhanced abbreviated MRI provided a sensitivity of 0.92 (95% CI: 0.62, 1.00), a specificity of 0.89 (95% CI: 0.82, 0.94), an NPV of 0.99 (95% CI: 0.94, 0.99), a PPV of 0.48 (95% CI: 0.27, 0.69), and an accuracy of 0.90 (95% CI: 0.83, 0.94).

Follow-up Abbreviated MRI Surveillance

Of the 306 patients with a non-positive baseline gadoxetate-enhanced abbreviated MRI, 163 patients underwent a total of 310 follow-up abbreviated MRI examinations during the study period. The interval between the first and second gadoxetate-enhanced abbreviated MRI examinations averaged 8.8 months (Fig 5a), then dropped to between 5.0 and 7.1 months on subsequent rounds of surveillance, with details provided in Figure 5.

After the baseline gadoxetate-enhanced abbreviated MRI, the proportion of positive examinations declined with subsequent rounds of surveillance (Fig 5b): 3.7% (six of 163), 2.3% (two of 86), and 2.3% (one of 44) in the second, third, and fourth rounds, respectively. The proportion of positive or subthreshold studies dropped to 6.1% (10 of 163) in the second round of

Table 4: Causes of 19 Inadequate Examinations

Reason for Inadequate Examination*	No. of Patients
Impaired hepatobiliary phase uptake of gadoxetate	15 (79)
Motion artifact	3 (16)
Dielectric artifact from ascites	2 (11)
Not specified in report	1 (5)

Note.—Data in parentheses are percentages.
* Two examinations were limited for more than one reason.

surveillance, then remained stable at 5.8% (five of 86) and 6.8% (three of 44) over the third and fourth rounds. No positive or subthreshold studies were reported in the fifth round of surveillance, noting a small sample size of 17 patients.

Discussion

In this retrospective study with cross-sectional and longitudinal components, we described our preliminary clinical experience with gadoxetate-enhanced abbreviated MRI as a clinical surveillance method for HCC, showed the feasibility of applying gadoxetate-enhanced abbreviated MRI-based surveillance at the institutional level with a high diagnostic adequacy rate, and provided a preliminary estimate of the detection accuracy of baseline gadoxetate-enhanced abbreviated MRI in at-risk patients. Our cancer detection rate was 37 HCCs per 1000 gadoxetate-enhanced abbreviated MRI examinations. Most patients had cirrhosis (93%), with the most common etiologies being HCV, alcohol, and NAFLD. This distribution agreed with recently reported demographics data for the cirrhotic population in the United States (28).

In a subcohort of 141 patients, we found that the prospectively issued clinical gadoxetate-enhanced abbreviated MRI reports provided high accuracy for HCC detection, with 91% sensitivity, 92% specificity, and 99% NPV, despite the substantial frequency of factors that plausibly could reduce lesion visualization, such as liver parenchymal heterogeneity (59%), ascites (18%), and impaired HBP enhancement (13%). The PPV was 48%, similar to the 54% PPV recently reported for multiphase MRI (29). Prior work has shown that simulated
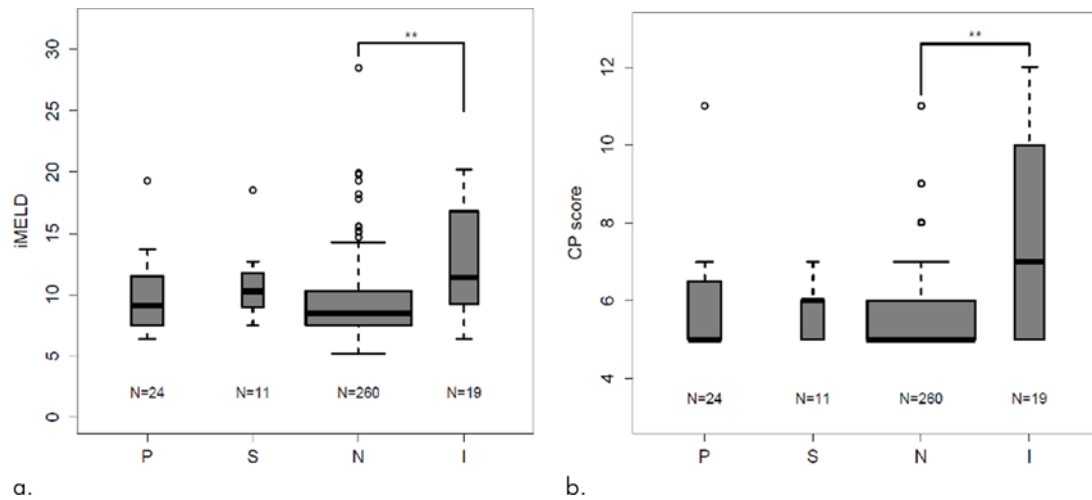
Figure 3: Inadequate baseline abbreviated MRI examination associated with higher integrated Model for End-stage Liver Disease (iMELD) and Child-Pugh (CP) scores: iMELD scores and CP scores were tabulated from laboratory data acquired within 6 months of baseline abbreviated MRI. **(a)** Box-and-whisker plot shows the mean iMELD score for patients with inadequate baseline gadoxetate-enhanced abbreviated MRI was significantly higher than the mean score of patients with negative baseline scans. A similar trend was noted between negative and both positive and subthreshold baseline studies but this failed to reach statistical significance. No significant difference existed between the positive, negative, and subthreshold groups. **(b)** Box-and-whisker plot show the mean CP score for patients with inadequate baseline gadoxetate-enhanced abbreviated MRI was significantly higher than the mean score of patients with negative baseline scans. A similar trend was noted between negative and both positive and subthreshold baseline studies, but this failed to reach statistical significance. No significant difference existed between the positive, negative, and subthreshold groups. I = inadequate baseline gadoxetate-enhanced abbreviated MRI, N = negative baseline gadoxetate-enhanced abbreviated MRI, P = positive baseline gadoxetate-enhanced abbreviated MRI, S = subthreshold baseline abbreviated MRI. ** = P < .01.

gadoxetate-enhanced abbreviated MRI can depict HCC lesions larger than 10 mm with a sensitivity of greater than 85% on a per-lesion basis (12), similar to our findings. The PPV of 48% was reasonable for a screening examination, although more detailed analyses of cost will be needed. It is likely that areas of fibrosis and dysplastic nodules both contributed to the number of false-positive cases, and further research is needed to refine the interpretation criteria to reduce false-positive readings. The addition of subthreshold examinations (presence of lesions < 10 mm) to positive studies (lesion size ≥ 10 mm) did not increase test sensitivity but did decrease both specificity and accuracy in the current study. This finding suggested that patients with subthreshold examinations continue surveillance imaging, which is our current institutional practice, rather than moving to multiphase CT or MRI. Our a priori plan for assessment of gadoxetate-enhanced abbreviated MRI performance metrics included inadequate examinations as part of the negative examination category. The motivation for this approach was founded on two key points: *(a)* This was a surveillance examination, and thus we considered it to have failed if it did not depict a cancer that was present at the time of the examination irrespective of whether the reason was technical error, biologic factors, or an error in human perception; and *(b)* we were concerned that a priori removal of inadequate examinations would introduce a bias (eg, by falsely elevating estimated sensitivity if there was a tumor present on one of the inadequate studies). However, all inadequate studies were ultimately classified as HCC negative (*n* = 15) or indeterminate (*n* = 4); thus, we also provided assessment of gadoxetate-enhanced abbreviated MRI performance with inadequate studies excluded, resulting in slight decreases in specificity, accuracy, and NPV.

At least nine of the 11 patients with HCC detected with gadoxetate-enhanced abbreviated MRI had potentially curable disease. In addition, one of the remaining two met the University of California San Francisco criteria for liver transplantation (30) at the time of diagnosis. The final patient likely had curable disease, but the lesion was missed at call-back multiphase MRI at least partially because of arterial phase mistiming. The patient was lost to follow-up before returning over a year later with incurable disease (see details in Table E1 [supplement]). Thus, our initial experience was that gadoxetate-enhanced abbreviated MRI can depict early and potentially curable disease in a surveillance population. Our preliminary sensitivity of 91% compares favorably with a recent meta-analysis that demonstrated a 47% sensitivity for US in the detection of early HCC (95% CI: 33%, 61%) (7).

The prevalence of HCC at baseline was 8.6%, which was higher than expected, given that the estimated annual incidence of HCC in cirrhosis generally ranges from 1%–6% (31–33). One possible explanation is that we excluded from the accuracy analysis 62 patients who had an additional 1 year or more of negative gadoxetate-enhanced abbreviated MRI surveillance without additional liver imaging (gadoxetate-enhanced abbreviated MRI results were not included in our composite reference standard). In addition, because patients with compromised US-based surveillance were the ones to undergo gadoxetate-enhanced abbreviated MRI preferentially, our cohort may have had more advanced cirrhosis than a typical surveillance population, which potentially could have increased the prevalence of HCC (34).

Liver function is known to affect image quality and thus diagnostic adequacy. In our study, the most common reason cited for inadequacy of gadoxetate-enhanced abbreviated MRI

was impaired HBP enhancement (15 of 19). We found that patients with inadequate examinations had significantly higher mean iMELD and Child-Pugh scores, suggesting that poor liver function contributed to technical inadequacy. Patients with inadequate examinations were also more likely to have ascites, impaired HBP uptake, and liver parenchymal heterogeneity. Despite these potential challenges and even though gadoxetate-enhanced abbreviated MRI was performed preferentially in patients with compromised US screening because of obesity, steatosis, parenchymal heterogeneity, or other factors, the adequacy rate (94.2%) was high in the 330 baseline examinations. Notably, the determination of gadoxetate-enhanced abbreviated MRI candidacy was made by the ordering hepatologist; thus, we could not assess the actual rate of failed US screening.

A high rate of diagnostic adequacy is critical to the cost-effectiveness of MRI-based surveillance. The expectation was that gadoxetate-enhanced abbreviated MRI would be charged at a reduced rate (our institution applies a 50% charge reduction for abbreviated MRI, as explained previously) because it requires significantly less imaging time (15 minutes or less in our experience) and has a simplified workflow (patients do not have to have contrast material injected while they are in the imaging system). However, nondiagnostic imaging will drive up costs, thus countering any potential cost savings. Previous work has suggested that gadoxetate-enhanced abbreviated MRI could offer cost savings of up to 49% compared with conventional methods (10). More recently, a comprehensive cost-utility assessment using various iterations of US, CT, and MRI-based strategies for HCC surveillance found that abbreviated MRI might be the most cost-effective in the setting of suboptimal compliance (19), the most likely real-world scenario. Prospective studies directly comparing the accuracy and cost-effectiveness of gadoxetate-enhanced abbreviated MRI with other methods, including US and dynamic abbreviated MRI using extracellular agents, are needed.

The average surveillance interval for the 163 patients who underwent multiple gadoxetate-enhanced abbreviated MRI examinations was 8.8 months. Existing guidelines from the American Association for the Study of Liver Diseases and the European Association for the Study of the Liver recommend surveillance with US with or without serum α-fetoprotein every 6 months (21,23). Despite our extended surveillance interval, there was no evidence that the number of positive studies increased with subsequent rounds of imaging. On the contrary, there was a trend toward declining numbers of positive examinations with each round of surveillance, possibly reflecting the high sensitivity of gadoxetate-enhanced abbreviated MRI. These findings suggest that an extended surveillance interval may be appropriate for gadoxetate-enhanced abbreviated MRI, with the potential to decrease cost and possibly to improve compliance, which may have implications in outcomes (35). Future studies are needed to confirm these potential benefits. Declining cancer detection rates between prevalence and incidence imaging have previously been observed with breast MRI, where widened screening intervals have also been proposed (36).

Our single-center retrospective study had limitations. Further studies will be needed to determine how these results apply in regions with different racial and liver disease demographics.
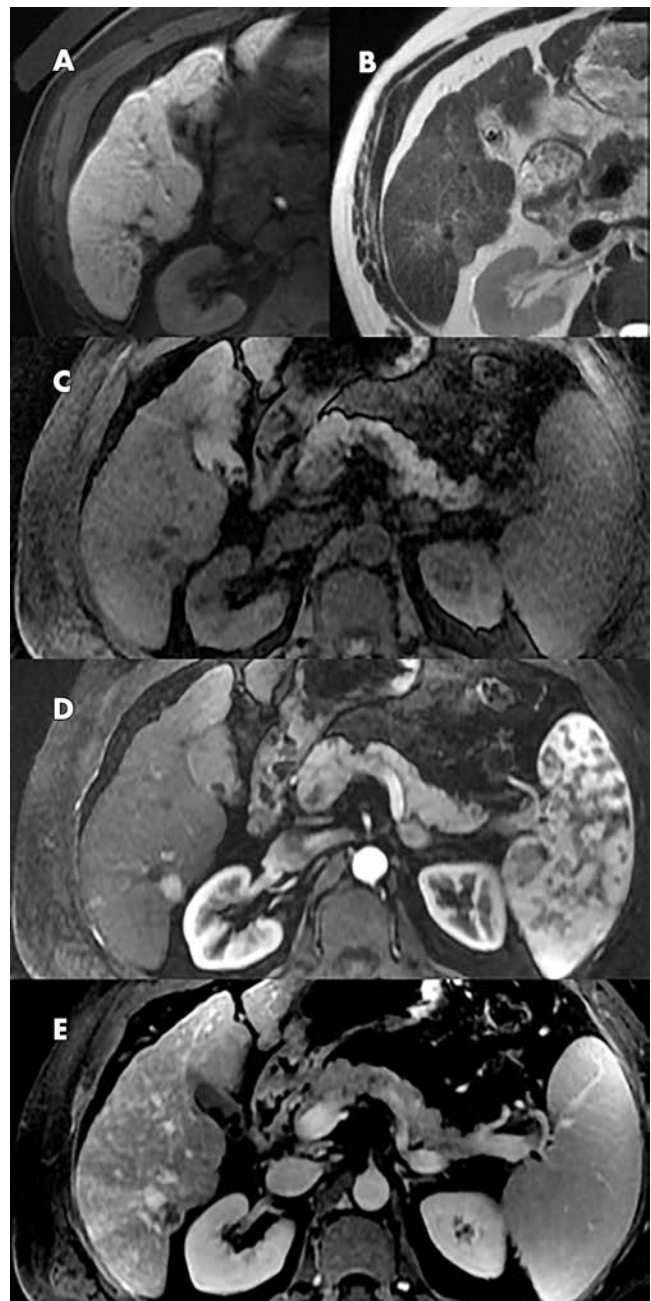

Figure 4: Hepatocellular carcinoma (HCC) detected with gadoxetate-enhanced abbreviated MRI screening. Positive gadoxetate-enhanced abbreviated MRI with Liver Imaging Reporting and Data System (LI-RADS) 5 observation at follow-up diagnostic MRI: gadoxetate-enhanced abbreviated MRI study, A, B; 15-mm hepatic segment VI lesion demonstrates hypointensity on T1-weighted three-dimensional gradient-echo fat-suppressed images acquired 20 minutes following administration of 0.025 mmol/kg gadoxetic disodium, A, and mild hyperintensity on T2-weighted single-shot fast spin-echo image. B, Diagnostic MRI 1 month later, C–E, shows a 15-mm lesion with late arterial hyperenhancement on T1-weighted three-dimensional gradient-echo fat-suppressed imaging following administration of extracellular contrast agent. D, with washout and capsule appearance. E, The observation was categorized as LI-RADS 5 (definite HCC).

We used a composite reference standard, with a large number of patients lost to follow-up. Clinically significant tumors may have been missed by the reference standard which could introduce verification bias, potentially leading to overestimation of gadoxetate-enhanced abbreviated MRI diagnostic performance.

Table 5: HCC Detection Performance of Baseline Gadoxetate-enhanced Abbreviated MRI

Parameter	Gadoxetate-enhanced Abbreviated MRI Classified as Positive if Examination Was Reported as Positive	Gadoxetate-enhanced Abbreviated MRI Classified as Positive if Examination Was Reported as Positive or Subthreshold	Gadoxetate-enhanced Abbreviated MRI Classified as Positive if Examination was Reported as Positive (Inadequate Examinations Removed)
Sensitivity (%)	92 (11/12) [62, 100]	92 (11/12) [62, 100]	92 (11/12) [62, 100]
Specificity (%)	91 (117/129) [84, 95]	85 (109/129) [77, 90]	89 (102/114) [82, 94]
Positive predictive value (%)	48 (11/23) [27, 69]	36 (11/31) [19, 55]	48 (11/23) [27, 69]
Negative predictive value (%)	99 (117/118) [95, 100]	99 (109/110) (95, 100)	99 (102/103) [94, 100]
Accuracy (%)	91 (128/141) [85, 95]	85 (120/141) [78, 91]	90 (113/126) [83, 94]
Cancer detection rate	37 HCCs/1000 examinations	37 HCCs/1000 examinations	37 HCCs/1000 examinations

Note.—Unless otherwise indicated, data are point estimates, numerator/denominator in parentheses, and exact binomial 95% confidence intervals in brackets. Values are based on data from Tables 3 and 4. HCC = hepatocellular carcinoma.
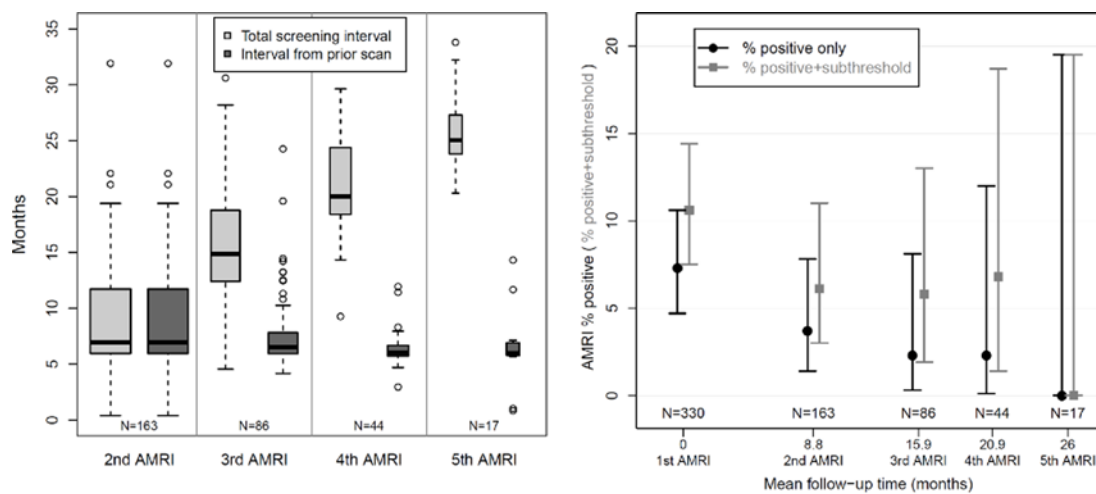
a.

b.

Figure 5: Surveillance results. **(a)** Boxplot shows surveillance interval data from the 163 patients who underwent at least one surveillance gadoxetate-enhanced abbreviated MRI (AMRI) after the baseline examination. The box plots show the median (solid horizontal bar), second and third quartile (solid box), and standard deviation (error bars) of the follow-up intervals between examinations for a given round of surveillance. The width of the plot is proportional to the number of studies in a given group, which is also listed at the bottom of the graph. Light gray represents the total interval from baseline examination, and dark gray represents the mean interval from the prior examination. **(b)** Graphic representation of the rate of positive examinations (black circles) or positive-plus-subthreshold examinations (gray squares) during a given round of gadoxetate-enhanced abbreviated MRI surveillance. The y-axis represents the percentage of studies in a group that were positive ± subthreshold. The x-axis represents the mean number of months between the first (baseline) examination and each subsequent round of surveillance. The number of studies in a given group is listed along the lower portion of the graph. There were 330 patients in the cohort who underwent a baseline (first) gadoxetate-enhanced abbreviated MRI examination, 163 who underwent a second examination, and so on. Error bars = lower and upper bounds of the 95% confidence interval.

Our choice of 1 year of follow-up for our composite reference standard was an attempt to minimize that risk. The exclusion from the accuracy analysis of patients whose only follow-up was gadoxetate-enhanced abbreviated MRI may have inflated the sensitivity estimation (because some of the patients may have had missed HCC) while also decreasing the estimated specificity and NPV. Our study was descriptive, did not compare gadoxetate-enhanced abbreviated MRI with other screening methods, such as US or alternative abbreviated MRI approaches, and did not include a cost-effectiveness analysis. Nor did these data assess outcome parameters such as diagnostic yield, false-referral rate, and the rate of unnecessary procedures as well as any associated complications. Our current practice is to report hyperintense

nodules as negative unless they have other suspicious imaging features, such as a nodule-in-nodule appearance. In our experience, these observations were far more likely to be benign and we suspected that including them would have significantly degraded our PPV and accuracy with minimal clinical yield. However, it is well established that HCC can be iso- or hyperintense at HBP imaging (37); thus, as the protocol was implemented, these lesions would not trigger call-back multiphase imaging, which is a theoretical limitation of the technique. Finally, more than half of the patients were lost to follow-up, which may have introduced errors in the reported diagnostic performance and limited the potential health benefit of surveillance. Noncompliance is a well-known and important limitation of all HCC surveillance

strategies in the United States (38–40), and strategies to improve compliance are urgently needed.

In summary, gadoxetate-enhanced abbreviated MRI is a rapid protocol aimed at reducing the cost and increasing the throughput of MRI-based HCC surveillance. Our preliminary experience suggested that gadoxetate-enhanced abbreviated MRI can be implemented clinically with high diagnostic adequacy in the setting of compromised US surveillance. Preliminary analysis of a subcohort of 141 patients demonstrated high sensitivity and NPV in detecting HCC in high-risk patients when interpreted prospectively on a subspecialty clinical service, but as with other HCC surveillance programs, there is a high loss-to-follow-up rate. Although rates of HCV-related cirrhosis are likely to decline in the coming decades, the rise of nonalcoholic steatohepatitis (41) and alcoholic cirrhosis (42) means that HCC surveillance will remain a clinically relevant issue for the foreseeable future. Rapid acquisition lower-cost MRI methods, such as gadoxetate-enhanced abbreviated MRI, may provide a viable approach for HCC surveillance in high-risk patients, especially those with compromised US screening.

References

1. McGlynn KA, Petrick JL, London WT. Global epidemiology of hepatocellular carcinoma: an emphasis on demographic and regional variability. Clin Liver Dis 2015;19(2):223–238.
2. Choi JY, Lee JM, Sirlin CB. CT and MR imaging diagnosis and staging of hepatocellular carcinoma: part I. Development, growth, and spread: key pathologic and imaging aspects. Radiology 2014;272(3):635–654.
3. Choi JY, Lee JM, Sirlin CB. CT and MR imaging diagnosis and staging of hepatocellular carcinoma: part II. Extracellular agents, hepatobiliary agents, and ancillary imaging features. Radiology 2014;273(1):30–50.
4. Singal A, Volk ML, Waljee A, et al. Meta-analysis: surveillance with ultrasound for early-stage hepatocellular carcinoma in patients with cirrhosis. Aliment Pharmacol Ther 2009;30(1):37–47.
5. Balogh J, Victor D 3rd, Asham EH, et al. Hepatocellular carcinoma: a review. J Hepatocell Carcinoma 2016;3:41–53.
6. Zhang BH, Yang BH, Tang ZY. Randomized controlled trial of screening for hepatocellular carcinoma. J Cancer Res Clin Oncol 2004;130(7):417–422.
7. Tzartzeva K, Obi J, Rich NE, et al. Surveillance imaging and alpha fetoprotein for early detection of hepatocellular carcinoma in patients with cirrhosis: a meta-analysis. Gastroenterology 2018;154(6):1706–1718.e1.
8. Colli A, Fraquelli M, Casazza G, et al. Accuracy of ultrasonography, spiral CT, magnetic resonance, and alpha-fetoprotein in diagnosing hepatocellular carcinoma: a systematic review. Am J Gastroenterol 2006;101(3):513–523.
9. Lee JY, Huo EJ, Weinstein S, et al. Evaluation of an abbreviated screening MRI protocol for patients at risk for hepatocellular carcinoma. Abdom Radiol (NY) 2018;43(7):1627–1633.
10. Besa C, Lewis S, Pandharipande PV, et al. Hepatocellular carcinoma detection: diagnostic performance of a simulated abbreviated MRI protocol combining diffusion-weighted and T1-weighted imaging at the delayed phase post gadoxetic acid. Abdom Radiol. 2017;42(1):179–190.
11. Marks RM, Ryan A, Heba ER, et al. Diagnostic Per-Patient Accuracy of an Abbreviated Hepatobiliary Phase Gadoxetic Acid–Enhanced MRI for Hepatocellular Carcinoma Surveillance. American Journal of Roentgenology. 2015;204(3):527–535.
12. Tillman BG, Gorman JD, Hru JM, et al. Diagnostic per-lesion performance of a simulated gadoxetate disodium-enhanceddabbreviated MRI protocol for hepatocellular carcinoma screening. Clinical Radiology. 2018;73(5):485–493.
13. Kuhl CK, Schrading S, Strobel K, Schild HH, Hilgers RD, Bieling HB. Abbreviated breast magnetic resonance imaging (MRI): first postcontrast subtracted images and maximum-intensity projection-a novel approach to breast cancer screening with MRI. J Clin Oncol 2014;32(22):2304–2310.
14. Ahn SS, Kim MJ, Lim JS, Hong HS, Chung YE, Choi JY. Added value of gadoxetic acid-enhanced hepatobiliary phase MR imaging in the diagnosis of hepatocellular carcinoma. Radiology 2010;255(2):459–466.
15. Ueno A, Masugi Y, Yamazaki K, et al. OATP1B3 expression is strongly associated with Wnt/β-catenin signalling and represents the transporter of gadoxetic acid in hepatocellular carcinoma. J Hepatol 2014;61(5):1080–1087.
16. Taouli B, Koh DM. Diffusion-weighted MR imaging of the liver. Radiology 2010;254(1):47–66.
17. Park MS, Kim S, Patel J, et al. Hepatocellular carcinoma: detection with diffusion-weighted versus contrast-enhanced magnetic resonance imaging in pretransplant patients. Hepatology 2012;56(1):140–148.
18. Semelka RC, Brown ED, Ascher SM, et al. Hepatic hemangiomas: a multi-institutional study of appearance on T2-weighted and serial gadolinium-enhanced gradient-echo MR images. Radiology 1994;192(2):401–406.
19. Lima PH, Fan B, Bérubé J, et al. Cost-utility analysis of imaging for surveillance and diagnosis of hepatocellular carcinoma. AJR Am J Roentgenol 2019 Apr 17:1–9. [Epub ahead of print].
20. Elsayes KM, Hooker JC, Agrons MM, et al. 2017 Version of LI-RADS for CT and MR imaging: an update. RadioGraphics 2017;37(7):1994–2017.
21. Heimbach JK, Kulik LM, Finn RS, et al. AASLD guidelines for the treatment of hepatocellular carcinoma. Hepatology 2018;67(1):358–380.
22. Omata M, Cheng AL, Kokudo N, et al. Asia-Pacific clinical practice guidelines on the management of hepatocellular carcinoma: a 2017 update. Hepatol Int 2017;11(4):317–370.
23. European Association for Study of Liver; European Organisation for Research and Treatment of Cancer. EASL-EORTC clinical practice guidelines: management of hepatocellular carcinoma. Eur J Cancer 2012;48(5):599–641.
24. ACR LI-RADS v2014. https://www.acr.org/Clinical-Resources/Reporting-and-Data-Systems/LI-RADS/LI-RADS-v2014. Accessed June 20, 2019.
25. LI-RADS. https://www.acr.org/Clinical-Resources/Reporting-and-Data-Systems/LI-RADS. Accessed June 20, 2019.
26. Luca A, Angermayr B, Bertolini G, et al. An integrated MELD model including serum sodium and age improves the prediction of early mortality in patients with cirrhosis. Liver Transpl 2007;13(8):1174–1180.

27. Mazzaferro V, Regalia E, Doci R, et al. Liver transplantation for the treatment of small hepatocellular carcinomas in patients with cirrhosis. N Engl J Med 1996;334(11):693–699.

28. Scaglione S, Kliethermes S, Cao G, et al. The epidemiology of cirrhosis in the United States: a population-based study. J Clin Gastroenterol 2015;49(8):690–696.

29. Kim SY, An J, Lim YS, et al. MRI with liver-specific contrast for surveillance of patients with cirrhosis at high risk of hepatocellular carcinoma. JAMA Oncol 2017;3(4):456–463.

30. Yao FY, Ferrell L, Bass NM, et al. Liver transplantation for hepatocellular carcinoma: expansion of the tumor size limits does not adversely impact survival. Hepatology 2001;33(6):1394–1403.

31. Kanwal F, Hoang T, Kramer JR, et al. Increasing prevalence of HCC and cirrhosis in patients with chronic hepatitis C virus infection. Gastroenterology 2011;140(4):1182–1188.e1.

32. Pateron D, Ganne N, Trinchet JC, et al. Prospective study of screening for hepatocellular carcinoma in Caucasian patients with cirrhosis. J Hepatol 1994;20(1):65–71.

33. Raffetti E, Fattovich G, Donato F. Incidence of hepatocellular carcinoma in untreated subjects with chronic hepatitis B: a systematic review and meta-analysis. Liver Int 2016;36(9):1239–1251.

34. Nakagomi R, Tateishi R, Masuzaki R, et al. Liver stiffness measurements in chronic hepatitis C: treatment evaluation and risk assessment. J Gastroenterol Hepatol 2019;34(5):921–928.

35. Costentin CE, Layese R, Bourcier V, et al. Compliance with hepatocellular carcinoma surveillance guidelines associated with increased lead-time adjusted survival of patients with compensated viral cirrhosis: a multi-center cohort study. Gastroenterology 2018;155(2):431–442.e10.

36. Kuhl CK, Strobel K, Bieling H, Leutner C, Schild HH, Schrading S. Supplemental breast MR imaging screening of women with average risk of breast cancer. Radiology 2017;283(2):361–370.

37. Kitao A, Zen Y, Matsui O, et al. Hepatocellular carcinoma: signal intensity at gadoxetic acid-enhanced MR Imaging--correlation with molecular transporters and histopathologic features. Radiology 2010;256(3):817–826.

38. Goldberg DS, Valderrama A, Kamalakar R, Sangsiry SS, Babajanyan S, Lewis JD. Hepatocellular carcinoma surveillance among cirrhotic patients with commercial health insurance. J Clin Gastroenterol 2016;50(3):258–265.

39. Singal AG, Tiro J, Li X, Adams-Huet B, Chubak J. Hepatocellular carcinoma surveillance among patients with cirrhosis in a population-based integrated health care delivery system. J Clin Gastroenterol 2017;51(7):650–655.

40. Goldberg DS, Taddei TH, Serper M, et al. Identifying barriers to hepatocellular carcinoma surveillance in a national sample of patients with cirrhosis. Hepatology 2017;65(3):864–874.

41. Estes C, Anstee QM, Arias-Loste MT, et al. Modeling NAFLD disease burden in China, France, Germany, Italy, Japan, Spain, United Kingdom, and United States for the period 2016-2030. J Hepatol 2018;69(4):896–904.

42. Pimpin L, Cortez-Pinto H, Negro F, et al. Burden of liver disease in Europe: epidemiology and analysis of risk factors to identify prevention policies. J Hepatol 2018;69(3):718–735.